



HAL
open science

Impact of control rod position and homogenization on sodium void effect in CFV-type SFR

M. Andersson, H. Nylen, D. Blanchet, R. Jacqmin

► To cite this version:

M. Andersson, H. Nylen, D. Blanchet, R. Jacqmin. Impact of control rod position and homogenization on sodium void effect in CFV-type SFR. PHYSOR 2016, May 2017, Sun Valley, United States. pp.2658-2667. cea-02431802

HAL Id: cea-02431802

<https://cea.hal.science/cea-02431802>

Submitted on 8 Jan 2020

HAL is a multi-disciplinary open access archive for the deposit and dissemination of scientific research documents, whether they are published or not. The documents may come from teaching and research institutions in France or abroad, or from public or private research centers.

L'archive ouverte pluridisciplinaire **HAL**, est destinée au dépôt et à la diffusion de documents scientifiques de niveau recherche, publiés ou non, émanant des établissements d'enseignement et de recherche français ou étrangers, des laboratoires publics ou privés.

IMPACT OF CONTROL ROD POSITION AND HOMOGENIZATION ON SODIUM VOID EFFECT IN CFV-TYPE SFR

M. Andersson and H. Nylén

Chalmers University of Technology, Department of Physics,
Division of Subatomic and Plasma Physics,
SE-412 96 Gothenburg, Sweden
andmika@chalmers.se
henrik@nephy.chalmers.se

D. Blanchet and R. Jacqmin

CEA, DEN, DER
F-13108 Saint-Paul-lez-Durance, France.
david.blanchet@cea.fr
robert.jacqmin@cea.fr

ABSTRACT

In complex innovative fast reactor concepts, fairly detailed core modeling is essential for reliable safety analysis during severe accident scenarios. The CFV core with its axially heterogeneous design, has a negative sodium void reactivity effect, a favorable feature which increases the inherent system safety in case of sodium boiling. In this work, we studied the impact that the control rod homogenization model used, and the control rod position, have on the sodium void-reactivity effect and the control rod worth, in the case of a voided CFV core. Three different control rod homogenization models were studied, the traditional *2D* equivalence procedure, and two models based on a *3D* equivalence procedure, taking into account the axial heterogeneity of the CFV core. It was found that the impact of control rod homogenization has a negligible effect on the sodium void reactivity effect. However, between different control rod positions, a difference of up to 1\$ in the sodium void reactivity effect was found, hence the control rod position has to be carefully considered when calculating the sodium void reactivity effect. For the control rod worth in a voided CFV core, the traditional *2D* procedure, could lead to discrepancies of up to 11% for control rod positions at the top of the core. These discrepancies could be much reduced by control rod homogenization with the *3D* equivalence procedure. For the total control rod worth, all models and procedures produced results within the desired error margin of $\pm 5\%$.

Key Words: **SFR, Control Rod, Void Reactivity Effect, ASTRID**

1. INTRODUCTION

Among the various Gen-IV reactors, advanced sodium-cooled fast reactors (SFRs), derived from proven technology and having inherent safety features, are seen as promising candidates for replacing LWRs

in a future transition to sustainable energy systems [1]. A number of these innovative SFRs are under study in the world, and one of those is the Advanced Sodium Technological Reactor for Industrial Demonstration (ASTRID) project in France [2].

In the preliminary design studies of ASTRID, an axially heterogeneous core has been proposed as a means of achieving a low (i.e. slightly positive or negative) sodium void reactivity worth, compared with more conventional homogeneous core designs. This kind of low sodium-void-worth core is denoted as a CFV-type core (French acronym of *Cœur à Faible effet de Vide sodium*, meaning *Low sodium void effect core*), which includes two fissile zones axially, sandwiching an inner fertile blanket, and a sodium plenum above the core.

Accurate modeling of the typical assembly-sized B_4C control rods is a well-known challenge [3]. In SUPERPHENIX, large discrepancies of up to 25% were found between calculated and measured control rod worth (CRW) [4]. These discrepancies were caused by the use of the diffusion theory approximation combined with simple methods for control-rod homogenization. When improved homogenization methods were introduced [3], and when the diffusion approximation was replaced by more rigorous transport calculations, these discrepancies were reduced to $\pm 5\%$. Since these improved methods were based on a 2D geometry, their performance remains to be assessed for CFV-type cores, in particular if the previous error margin ($\pm 5\%$) can still be achieved.

The work reported here builds upon an earlier physics study [5], in which the impact of spectral changes on equivalent homogenized cross section was investigated in a one-dimensional model. This investigation has since been extended to 2D [6] and 3D [7] models, which included varying material environments around a control-rod subassembly. In the present paper, we focus on control rod homogenization in voided environments, and the impact that the control rod cross sections have on the CRW, in a voided CFV core. In addition, we investigate the impact of the control rod position on the total sodium void reactivity effect (SVRE).

2. CORE DESCRIPTION

In this study, we used a CFV core model based on a pre-conceptual design of the ASTRID reactor [8], which is a 1500 MW(thermal) SFR, designed so as to have a zero net breeding gain and a SVRE of -0.5 \$ at End of Cycle (EOC). The radial core map and the axial core alignment can be seen in Fig. 1. The two types of fuel subassemblies (inner and outer fuel) consist of 217 Mixed Oxide (MOX) fuel pins in a stainless steel cladding, with a plutonium content of 23.5 % for the inner fuel and 20 % for the outer fuel. The inner fuel subassemblies are axially heterogeneous (see Fig. 1), where a 25 cm lower fissile zone, a 20 cm inner fertile blanket, and a 35 cm upper fissile zone are stacked up. Above the active core, there are successively: a gas plenum, sodium plenum, and an upper neutron shield.

The shutdown system consists of two parts: 12 control shutdown system (CSD), and 6 diverse shutdown system (DSD). All control rods are based on the description in [9], where the control rod is

axially divided into four parts: the sodium rich follower, the lower boron enriched region of the absorber, an upper higher boron enriched absorber region, and the driver mechanism. In this study, the absorber section of both the CSDs and the DSDs have a total length of 80 cm. For the CSDs, the lower region is 60 cm, and consists of naturally enriched B_4C , while the upper region is 20 cm and consists of 48 % boron-10 enriched B_4C . For the DSDs, the lower region is 20 cm, and consists of 48 % boron-10 enriched B_4C , whereas the upper region is 60 cm, and consists of 90 % boron-10 enriched B_4C . The shutdown systems are schematically depicted in Fig. 1.

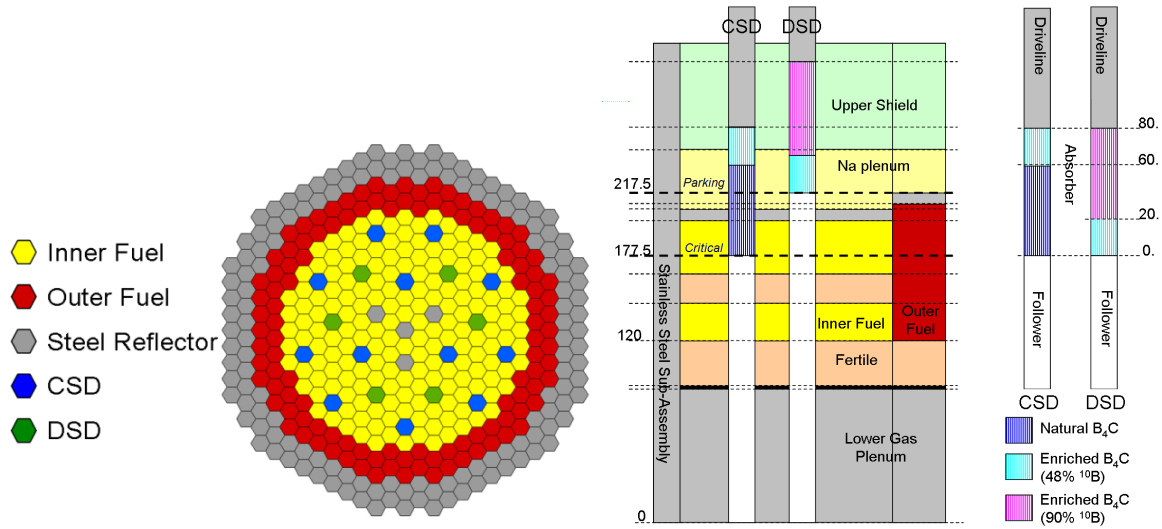


Figure 1. Left: the radial core map of the CFV core. Right: the axial alignment of the CFV core.

3. METHODOLOGY

In order to determine the SVRE, two 3D CFV core models are used: in the first model, the sodium is present (nominal density) in the entire core. In the second model, the sodium is voided (nominal density $\cdot 10^{-12}$) in regions inside, and above the "active core" (sodium plenum, gas plenum, fissile zones and the inner fertile blanket). The SVRE is calculated as:

$$SVRE = \rho_{void} - \rho_{nominal} \quad (1)$$

The SVRE values are calculated for varying control rod bank positions, to determine the impact the control-rod-cross sections, and the control-rod position, have on the SVRE, and how the voided conditions affects the CRW. The CRW is calculated as:

$$\rho_{CRW} = \rho_i - \rho_{ref} \quad (2)$$

where ρ_i is the reactivity at control rod position i , and ρ_{ref} is a reference position. The usual reference position is when the control rod is in its parking position, in the sodium plenum (see Fig. 1). However,

since the impact of the voided plenum is investigated, it was deemed preferable to consider instead another reference position, corresponding to the control rod fully withdrawn past the upper shield, therefore the control rod is fully replaced with a sodium follower. As a reference, a Monte Carlo model has been used, and the calculations were performed with Tripoli4 (T4) [10].

The calculations are performed for fresh core conditions at room temperature; this is mainly for simplicity reasons and to avoid possible ambiguities when comparing with separate Monte Carlo results. Therefore, no burnup, material expansions, or Doppler broadening are considered here. The worst case (least negative) for the SVRE is not at the beginning of life, but at the EOC. However, since this study focuses on the impact that the control-rod homogenization has on the SVRE, this aspect is disregarded. Also, for a complete evaluation, both boron and fuel burnups would have to be taken into account into the model [9]. In this paper, both the CRW and SVRE are presented in \$ with a value of the effective delayed neutron fraction $\beta_{eff} = 365$ pcm. The deterministic core calculations are performed with the VARIANT code [11] within the ERANOS code package [12], with a P3 angular approximation, and a convergence criteria on both k_{eff} and the fission source of $5 \cdot 10^{-5}$.

3.1. Control Rod Partitioning and Homogenization

Based on previous work [6, 7], the 80 cm control rod absorber is partitioned into 10 cm segments, each assigned a unique set of cross sections, taking into account the spectral shifts the control rod is experiencing in different environments (see Fig: 1). This is done to reduce the number of homogenizations needed, even though it was shown in [7] that a smaller partitioning would be required in some control rod positions. Similar to the conditions stated in [7], the following assumptions and approximations are made:

1. In the sodium plenum (both voided and non-voided), the cross sections are assumed not to change significantly farther than 10 cm away from the fissile zone, and the same cross-section set is used for all control-rod segments situated in the plenum.
2. When a segment is farther away than 5 cm from an environment interface (such as the fissile/plenum interface), the effect of that interface is neglected.
3. When no internal control-rod interface is present (as for the follower/absorber), the fissile/fertile interfaces are treated in the same way.

The method used for the control-rod homogenization in this study, i.e. the equivalence procedure, is based on the work by Rowlands and Eaton [3], which in turn is based on reactivity equivalence instead of simple reaction-rate preservation. This equivalence procedure utilizes two models of the control rod subassembly: one in which the absorber rods are heterogeneously described (explicit representation of all B₄C absorbers), and another model in which the control rod is homogeneously described. In both

models, the external control rod environment is homogeneously modeled. With these two models, relationships for the reactivity-equivalent homogeneous cross sections can be derived using perturbation theory, where the heterogeneous model corresponds to the reference case, and the homogeneous model the perturbed case. The capture cross sections can be calculated as:

$$\Sigma_{c,hom}^g = \frac{\int_V dV \Sigma_{c,het}^g \int_{(4\pi)} d^2\Omega \psi_{het}^g \psi_{hom}^{+g}}{\int_V dV \int_{(4\pi)} d^2\Omega \psi_{het}^g \psi_{hom}^{+g}} \quad (3)$$

and for the scattering cross sections:

$$\Sigma_{sl,hom}^{g \rightarrow g'} = \frac{\int_V dV \Sigma_{sl,het}^{g \rightarrow g'} \left(\int_{(4\pi)} d^2\Omega \psi_{l,het}^g \cdot \int_{(4\pi)} d^2\Omega \psi_{l,hom}^{+g'} \right)}{\int_V dV \left(\int_{(4\pi)} d^2\Omega \psi_{l,het}^g \cdot \int_{(4\pi)} d^2\Omega \psi_{l,hom}^{+g'} \right)} \quad (4)$$

where ψ_{het}^g is the direct neutron flux for the heterogeneous system, ψ_{hom}^{+g} the adjoint neutron flux for the homogeneous system, and $\Sigma_{x,het}^g$ the heterogeneous cross sections. As seen in Eq. (3) and (4), the equivalent homogeneous cross sections are dependent on the homogeneous flux, which in turn calls for an iterative solution procedure. Such a procedure was implemented in 3D (Cartesian X-Y-Z) geometry, in the PARIS platform [13], in order to be able to account for the different axial environments the control rod will experience, to be compared with the previous, more approximate (2D X-Y) solutions.

In the self-scattering cross sections of order zero, seen in Eq. (5), a minus sign can be found. This minus sign can, for some energy groups, give rise to negative scattering-cross sections, and alter the stability of the procedure.

$$\Sigma_{s0,hom}^{g \rightarrow g} = \frac{\int_V dV \Sigma_{s0,het}^{g \rightarrow g} \left(\int_{(4\pi)} d^2\Omega \psi_{het}^g \psi_{hom}^{+g} - \int_{(4\pi)} d^2\Omega \psi_{hom}^{+g} \cdot \int_{(4\pi)} d^2\Omega \psi_{het}^g \right)}{\int_V dV \left(\int_{(4\pi)} d^2\Omega \psi_{het}^g \psi_{hom}^{+g} - \int_{(4\pi)} d^2\Omega \psi_{hom}^{+g} \cdot \int_{(4\pi)} d^2\Omega \psi_{het}^g \right)} \quad (5)$$

To stabilize the procedure, a simple fix-up was introduced in the PARIS implementation taking the absolute values of the flux integrals in Eq. (5) as:

$$\Sigma_{s0,hom}^{g \rightarrow g} = \frac{\int_V dV \Sigma_{s0,het}^{g \rightarrow g} \left(\left| \int_{(4\pi)} d^2\Omega \psi_{het}^g \psi_{hom}^{+g} - \int_{(4\pi)} d^2\Omega \psi_{hom}^{+g} \cdot \int_{(4\pi)} d^2\Omega \psi_{het}^g \right| \right)}{\int_V dV \left(\left| \int_{(4\pi)} d^2\Omega \psi_{het}^g \psi_{hom}^{+g} - \int_{(4\pi)} d^2\Omega \psi_{hom}^{+g} \cdot \int_{(4\pi)} d^2\Omega \psi_{het}^g \right| \right)} \quad (6)$$

This absolute value will in some cases give rise to slightly larger self-scattering cross sections (especially for low energy groups), and the reactivity difference between the heterogeneous and the homogeneous systems will no longer be zero. This will lead to a redefinition of the convergence criteria for the equivalence procedure to $|\rho_{hom}^i - \rho_{hom}^{i-1}| < \epsilon$, instead of $|\rho_{het} - \rho_{hom}^i| < \epsilon$. However, this fix-up is expected to have a small impact on the overall results since it mostly affects the lower energy groups, where the neutron flux is low.

The heterogeneous 3D geometry consists of several (2D X-Y) models, in which the control rod is surrounded by a single homogeneous environment. To form the 3D environment, several of these X-Y sections are stacked, forming a 3D environment.

The homogenization calculations are performed with a 33 energy group structure [14], a S_4 discrete ordinate quadrature, discontinuous Galerkin spatial approximation and, a convergence criteria of 10^{-5} on the eigenvalue and 10^{-4} on the flux, performed with the PARIS code [13]. The convergence criteria on the equivalence procedure was set to 10 pcm.

3.2. Cases Investigated

In usual core-wide void-effect calculations, the sodium in the control-rod subassemblies is assumed to remain present in voided core conditions. In this study, in addition to the above assumption, the S-curve is calculated with three different sets of equivalent control rod cross sections, calculated by making the following approximations:

- The original procedure (denoted *ORG*), is where sodium is present in both the control rod and in the surrounding environments. *ORG* uses the original 2D (*X-Y*) version of the equivalence procedure, and is the classical way of generating control-rod-cross sections. For the SVRE, the same set of control-rod-cross sections are used for both the nominal and the voided cores.
- The new, 3D environment-corrected procedure (denoted *EC*), is calculated with the 3D version of the equivalence procedure, where as in *ORG*, the sodium is present in both the control rod and its environment. For the SVRE, the same set of control rod cross sections is used for both the nominal and voided cores.
- Voided environment (denoted *EC_{void}*), is where sodium is removed from the control rod surrounding environment, but remains present inside the control rod. In this case, for calculating the SVRE, the *EC* sets of cross sections are used for the nominal core, and the *EC_{void}* for the voided core.

The assumptions and approximations made in this and the previous section are required in order to reduce the memory requirements and calculation time of the homogenization, since 60 unique sets of homogeneous equivalent control-rod-cross sections are needed in this study to perform the S-curve calculations, for both nominal and voided cases.

4. RESULTS

4.1. Sodium Void Reactivity Effect

The SVRE for the three cases, and the T4 reference can be seen in Fig. 2, presented for the case where the whole CSD bank is moved. It can be seen in Fig. 2, that the difference between the three

deterministic cases investigated is very small, with a maximum discrepancy between the cases of 3% (corresponding to 0.09 \$). However, in Fig. 2, a bias between the deterministic calculations for the three cases and the T4 reference model, of about 1 \$, can be observed for all control rod positions. This constant bias was previously studied [15] with the conclusion that it is caused by errors arising from neutron leakage modeling.

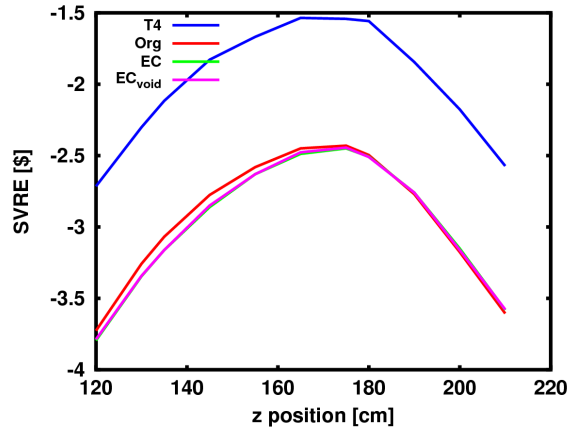


Figure 2. The SVRE presented for three cases, compared with T4 results.

It can be seen in Fig. 2, that the SVRE is highly dependent on the control rod position, with more than a 1 \$ difference between its minimum and maximum values. The least negative SVRE corresponds to control rod positions just below the critical position. The main contributor to the SVRE in the CFV core is the axial leakage through the voided sodium plenum to the upper neutron shield, where the neutrons can be absorbed, hence with increased leakage, a larger SVRE will be obtained. When the control rods are situated within the sodium plenum, the control rods act as an additional upper protection, reducing neutron scattering back into the core. With the control rods slightly inserted in the core, the neutron flux is pushed down in the core, causing a reduction in the leakage up through the sodium plenum, and thereby reducing the SVRE. However, when the control rods are further inserted into the core, the axial flux distribution flattens out again, allowing the neutrons to leak through the sodium plenum, increasing the SVRE.

4.2. Control Rod Worth

The integral CRW computed with T4 for the nominal and voided cores can be seen in Fig. 3 a and the corresponding differential CRW in Fig. 3 b, presented for the case where the whole CSD bank is moved. It can be seen in Fig. 3 b, that the differential CRW curve is slightly shifted, with the largest differential CRW further down in the core, in comparison with the nominal case, making the control rod in the voided situations less efficient at the top of the core. This shift is caused by the increased leakage through the voided plenum, thus comparatively fewer neutrons at the top of the active core are absorbed by boron. The difference in CRW between the three cases and the T4 reference, for the voided

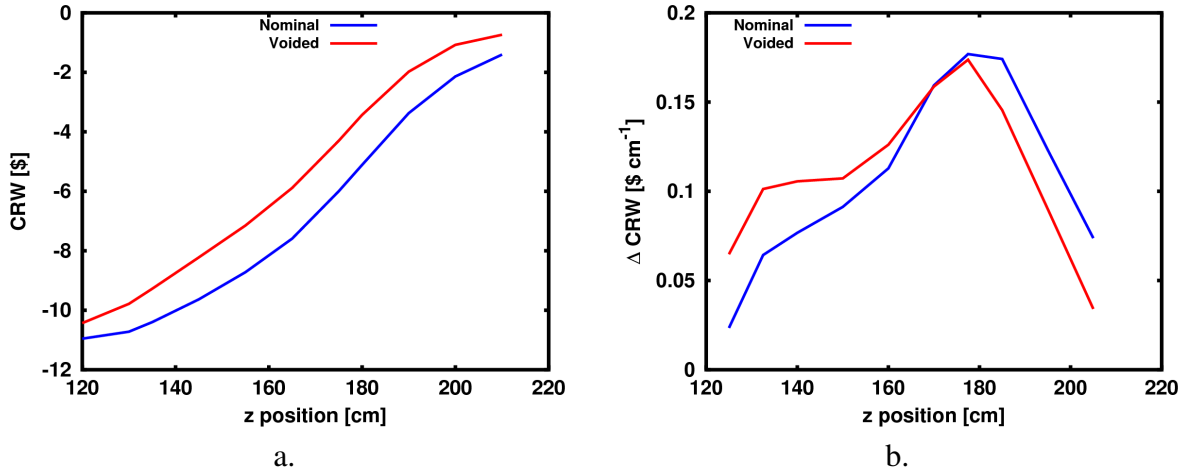


Figure 3. The integral (a) and differential (b) CRW T4 results, for the nominal and voided cases.

configuration, are compared in Fig. 4. The *ORG* approximation results in a less accurate prediction of the CRW, when slightly inserted into the core, with an underprediction of almost 11% ($0.25 \$ \pm 0.05 \$ (2\sigma)$). However, with the bulk of the control rod inserted, for the *ORG*, a better prediction in CRW is observed. The *EC* case improves the CRW prediction at the top of the core, with a maximum underprediction of 6%. With the correct environmental treatment in *EC_{void}*, the discrepancy at the top of the core is further reduced, to a maximum underprediction of 3%. However, it can be seen in both the *EC* and *EC_{void}* results, that in the parking position (210 cm), the discrepancy is greatly increased. This was studied in [7], and is a consequence of the fairly large 10 cm axial subdivision used in modeling the environment of the follower/absorber interface within the sodium plenum, for computing the equivalent cross sections. With a finer partitioning of the first 10 cm of the control rod at this position, the discrepancy can be reduced.

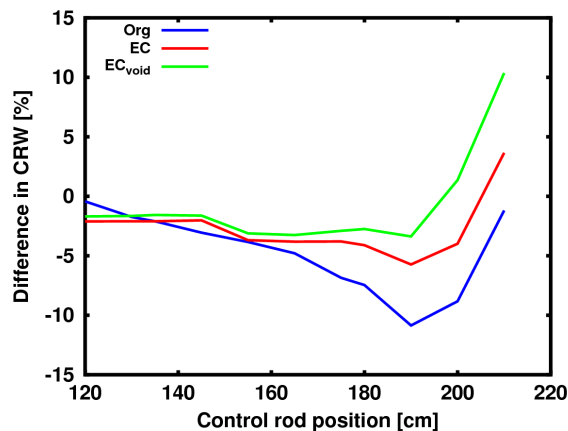


Figure 4. The CRW error as a function of control rod position, as computed with T4.

5. CONCLUSIONS

One of the main design parameters of the CFV core concept is the sodium void-reactivity effect (not to exceed $-0.5 \text{ \$}$ at EOC). With an axially heterogeneous design of such a core, a negative sodium void reactivity effect is achieved. In this work, for a voided CFV core, we have studied the effect that the control-rod cross sections, in different control rod positions, have on the control rod worth, as well as on the sodium void reactivity effect. The different control rod cross sections used, were either generated by the traditional $2D$ equivalence procedure, or an expanded $3D$ equivalence procedure, taking into account the axial heterogeneities of the CFV core and the control rod itself.

It was found that, for the sodium-void-reactivity effect, the control-rod cross sections have a very small impact, where the maximum difference between the traditional methodology and the $3D$ one is less than 3% ($0.09 \text{ \$}$). However, the position of the control rod has a much stronger impact, with differences of up to $1 \text{ \$}$ in the sodium void reactivity worth, the minimum value being reached when the control rod is inserted through the whole upper fissile zone. This implies that care should be taken when defining the sodium void reactivity worth, if it is to be calculated at the most penalizing control rod position, or fully inserted (as the control rods would be during an accident scenario).

For the control rod worth in a voided core, the traditional $2D$ equivalence procedure, at control rod positions close to the sodium plenum, underestimates the control rod worth by up to 11%. With the $3D$ equivalenced cross sections, these discrepancies were greatly reduced to a maximum deviation of 3%, but at high computational expense. However, the performance achieved with the traditional $2D$ procedure for the total control rod worth and the sodium void reactivity effect, is within the required error limits ($\pm 5\%$).

ACKNOWLEDGMENTS

This work was performed in a collaboration between Chalmers University of Technology, in Gothenburg Sweden, and the CEA in France. The project was financed by the Swedish Research Council (Grant No B0774801).

REFERENCES

- [1] OECD/NEA. *Technology Roadmap Update for Generation IV Nuclear Energy Systems. Technical report*, OECD/NEA (2002).
- [2] B. Fontaine *et al.* "The French R&D on SFR core design and ASTRID project." In: *Proceedings of GLOBAL*. Makuhari, Japan (2011).

- [3] J. Rowlands and C. Eaton. “The spatial averaging of cross sections for use in transport theory calculations with and application to control rod fine homogenisation.” In: *Specialists meeting on homogenisation methods in reactor physics*. Lugano, Switzerland (1978).
- [4] M. Giese, M. Carta, and J. West. “Measurement and predictions of control rod worth.” *Nucl. Sci. Eng*, **106**: pp. 18–29 (1990).
- [5] M. Andersson *et al.* “Influence of local spectral variations on control-rod homogenization in fast reactor environments.” *Nucl. Sci. Eng*, **181(2)**: pp. 204–215 (2015).
- [6] —. “Control rod homogenization in fast reactor environments. Part I: Classification of axial spectral regions.” *Nucl. Sci. Eng* (to be submitted).
- [7] —. “Control rod homogenization in fast reactor environments. Part II: A 3 dimensional assessment.” *Nucl. Sci. Eng* (to be submitted).
- [8] F. Varaine *et al.* “Pre-conceptual design study of ASTRID core.” In: *Proc. Int. Cong. on Advances in Nucl. Power Plants (ICAPP2012)*. American Nuclear Society, Chicago, Illinois (2012).
- [9] D. Blanchet and B. Fontaine. “Control rod depletion in sodium-cooled fast reactor: models and impact on reactivity control.” *Nucl. Sci. Eng*, **177**: pp. 260–274 (2014).
- [10] E. Brun *et al.* “Overview of TRIPOLI4 version 7 continuous energy monte varlo code.” In: *Proc. Int. Cong. on Advances in Nucl. Power Plants (ICAPP2011)*. ACM Press, Nice, France (2011).
- [11] C. B. Carrico, E. E. Lewis, and G. Palmiotti. “Three-dimensional variational nodal transport methods for cartesian, triangular, and hexagonal criticality calculations.” *Nucl. Sci. Eng*, **111(2)**: pp. 168–179 (1992).
- [12] G. Rimpault *et al.* “The ERANOS data and code system for fast reactor neutronic analyses.” In: *Proceedings of PHYSOR*. Seoul, South Korea (2002).
- [13] R. Le Tellier *et al.* “High-order discrete ordinate transport in hexagonal geometry: a new capability in ERANOS.” In: *21st International Conference on Transport Theory (ICTT-21)*. Torino, Italy (2009).
- [14] E. Sartori. *Standard energy group structures of cross section libraries for reactor shielding, reactor cell and fusion neutronics applications: VITAMIN-J, ECCO-33, ECCO-2000 and XMAS, JEF/DOC-315, Revision 3, NEA Data Bank*. Gif-sur-Yvette Cedex, France (1990).
- [15] P. Sciora *et al.* “Low void effect core design applied on 2400 MWth SFR reactor.” In: *Proceedings of ICAPP*. ACM Press, Nice, France (2011).